

## OPTIMIZATION OF PROCESS PARAMETERS IN MICRO MILLING OF $Ti_4Al_4Mo_2Sn$ USING NANO $Al_2O_3$ ADDITIVES BASED MINIMUM QUANTITY COOLING LUBRICATION

M. Nithyanandam<sup>1\*</sup>, I. Rahamathullah<sup>2</sup> and R. Ashok Raj<sup>3</sup>

<sup>1</sup>Department of Mechanical Engineering, Priyadarshini Engineering College, Vaniyambadi, Tamilnadu, India

<sup>2</sup>Department of Mechanical Engineering, Government College of Engineering, Srirangam, Trichy, Tamilnadu, India

<sup>3</sup>Department of Mechanical Engineering, J.J College of Engineering and Technology, Trichy, Tamilnadu, India

(Received February 3, 2022; Revised March 30, 2022; Accepted April 12 2022)

**ABSTRACT.** Aerospace and automotive industries employ  $Ti_4Al_4Mo_2Sn$  material in many applications due to its properties of better strength to weight ratio and high corrosion resistance.  $Ti_4Al_4Mo_2Sn$  finds itself difficult to cut materials due to its physical and chemical properties and is prone to more heat generation during machining. The more generation of heat affects the machined material surface quality and other related properties. In this investigation, the thermal conductivity and stability of  $Al_2O_3$ /Water based nanofluids are studied to select the best composition of nanofluid for transferring heat. The thermal conductivity and stability of the nanofluid for a duration of 30 days are computed by employing the KD2 thermal property meter and pH meter, respectively. Thermal conductivity and stability of the Water/4.5 vol.%  $Al_2O_3$  nanofluid are found to be better than other combination of nanofluids. In the present study, optimizing the micro milling process parameters on  $Ti_4Al_4Mo_2Sn$  material with Minimum quantity cooling lubrication (MQL) is focused. The input parameters selected for this micro milling process are spindle speed, feed rate, depth of cut and Water/4.5vol.%  $Al_2O_3$  nanofluid and the output parameters selected are cutting forces in X( $F_x$ ) and Y( $F_y$ ) directions, tool wear rate (TWR) and surface roughness (SR). The optimization is done with the help of grey relational analysis (GRA) by using L9 Orthogonal Array (OA) Taguchi design. The obtained sequence of influencing parameters are feed rate per tooth,  $Al_2O_3$ nanofluid, spindle speed and depth of cut. The percentage of grey relational grade (GRG) for prediction and experimental is 0.721 and 0.957. The percentage of improvement of GRG is 12.46.

**KEY WORDS:**  $Ti_4Al_4Mo_2Sn$ ,  $Al_2O_3$ , Thermal conductivity, Grey relational analysis, Grey relational grade

## INTRODUCTION

The better strength to weight ratio and high corrosion resistance properties of material enhances their usages in various applications of aerospace and automotive industries and this kind of material is very difficult to cut. It is suitable for fabricating engine discs, blades, shafts and casings of high pressure compressor blades and nozzle assemblies [1]. The tool life and machined surface roughness of the machined material are highly influenced by the high hardness and low thermal conductivity properties of the material. The machinability and production cost are significantly influenced by the design variables such as tool geometry, cutting velocity, coolant strategy, depth of cut and feed rate [2].

Hardened steels, titanium alloys and ceramics are materials that are difficult to cut. The optimization is done on the machining variables including coolant parameters for this kind of materials [1, 3]. High temperature and excessive heat are generated while machining hard materials. The excessive heat generation causes to surface integrity and enhanced tool wear [4, 5]. The nanofluids are widely used as coolant in machining applications which are formed by the dispersion of nanoparticle and the nanoparticle size is between 1-100 nm. The nanofluids enhance

\*Corresponding author. E-mail: [nithm280288@gmail.com](mailto:nithm280288@gmail.com)

This work is licensed under the Creative Commons Attribution 4.0 International License

the heat transfer of base fluids [6] and the thermal conductivity of the nanofluid is established by the volume fraction, particle size, particle shape, pH value and temperature [7, 8]. The thermal conductivity of nanofluids was determined with the help of transient hot wire method (THW) [9]. The smaller size of nano additives enhanced the heat transfer rate than the bigger size of nano particle [10]. The conventional method for eliminating the heat transfer is flood cooling in which more coolant gets wasted. Therefore, the minimum quantity coolant is employed to rectify this problem in flood cooling [11-13]. A low flank wear and surface integrity are achieved by the application of MQL. The MQL technique dissipates the heat quickly [14, 15]. The cutting forces on EN8 are minimized while using MWCNTs-MQL [16]. Genetic algorithm, analytical hierarchy process and grey relational analysis (GRA) are employed for multi objective parameter optimization [16, 17]. The influence of MQL is analyzed in the turning of Al7075 and Al2024 aluminium based alloys. A small quantity of fluid is atomized and mixed with high pressure compressor air and applied to the machining zone [18]. The performance of the Water/Al<sub>2</sub>O<sub>3</sub> nanofluid was analyzed in the aspect of heat transfer, but not focused on the implementation of nanofluid as a MQCL fluid on micromachining application. The additive particle shape is influenced by the thermal conductivity of the nanofluid [19-22]. There is no/limited work done on implementing the Water/Al<sub>2</sub>O<sub>3</sub> nanofluid with MQL technique during the machining of Ti<sub>4</sub>Al<sub>4</sub>Mo<sub>2</sub>Sn material. In this investigation, an attempt has been made to optimize the micro machining process parameters of Ti<sub>4</sub>Al<sub>4</sub>Mo<sub>2</sub>Sn material.

## EXPERIMENTAL

### *Materials*

The Ti<sub>4</sub>Al<sub>4</sub>Mo<sub>2</sub>Sn material is selected as the work material because of its high hardness, corrosion resistance, temperature resistance and fatigue resistance. The Vickers hardness test, tension test, compression test and salt spray corrosion test are conducted as per ASTM standard for determining the hardness, tensile strength, compressive strength and corrosion resistance of the Ti<sub>4</sub>Al<sub>4</sub>Mo<sub>2</sub>Sn material. The Ti<sub>4</sub>Al<sub>4</sub>Mo<sub>2</sub>Sn material has a Vickers hardness of 340 HV, a compressive strength of 1000 MPa, a tensile strength of 1100 MPa and a mass loss of 2 mg for the duration of 60 hours. As, it is difficult for a machining with high surface finish, the MQC method is implemented to dissipate the heat and improve the surface finish. The Ti<sub>4</sub>Al<sub>4</sub>Mo<sub>2</sub>Sn material has been widely employed in the fabrication of air frame forgings, compressor blade and discs. A high machining precision is needed for these applications and it can be obtained by micro machining. A higher heat is generated during the machining of Ti<sub>4</sub>Al<sub>4</sub>Mo<sub>2</sub>Sn and it causes a worst surface integrity and tool wear. Therefore, a micro machine and tool is employed for this investigation. The composition of the Ti<sub>4</sub>Al<sub>4</sub>Mo<sub>2</sub>Sn material is Al (4%), Sn (2%), Mo (4%), Si (0.5%), O<sub>2</sub> (0.17%), Fe (0.16%), C (0.04%), N<sub>2</sub> (0.02%), H<sub>2</sub> (0.014%) and Ti (Bal.%). The excessive heat generation is dissipated by a nanofluid with MQL technique. Al<sub>2</sub>O<sub>3</sub> with a particle size of 20 nm is selected as nano additives to produce the nanofluid. Ti<sub>4</sub>Al<sub>4</sub>Mo<sub>2</sub>Sn and Al<sub>2</sub>O<sub>3</sub> materials are acquired from Sigma-Alrich, USA. The average particle size of Al<sub>2</sub>O<sub>3</sub> is analyzed by employing the particle size analyzer (PSA) [23] The PSA is used to identify the particle size of Al<sub>2</sub>O<sub>3</sub> and the test results are 96.4% with 20 nm, 1.6% with 22 nm and 2% with 25 nm. So the average particle size of Al<sub>2</sub>O<sub>3</sub> additive is estimated as 20 nm. The presence of elements in Al<sub>2</sub>O<sub>3</sub> is computed with the help of energy dispersive X-ray analysis (EDAX). The microstructure of the Al<sub>2</sub>O<sub>3</sub> is studied with the help of scanning electron microscope (SEM) and transmission electron microscope (TEM). The water based nanofluids combinations are Water/1.5 vol.% Al<sub>2</sub>O<sub>3</sub>, Water/3 vol.% Al<sub>2</sub>O<sub>3</sub>, Water/4.5 vol.% Al<sub>2</sub>O<sub>3</sub> and Water/6 vol.% Al<sub>2</sub>O<sub>3</sub>. The nanofluids are prepared by a two-step method [24]. Water is mixed with different vol. % of nano additives by an AQUASONIC-50HT ultrasonic device for 60 minutes and it is subjected to a magnetic stirrer for 30 min. The dispersion is done at one hour with a sonic frequency of 20 kHz and an electric power

of 300 W. A uniform distribution of nano additives in the base fluid is achieved in this method. The microstructure of the Water/x vol.%  $\text{Al}_2\text{O}_3$  ( $x = 1.5, 3$  and  $4.5$ ) is studied with the help of SEM. The thermal conductivity and stability of the prepared nanofluids are determined with the help of KD2 thermal analyzer and pH meter [25].

#### *Taguchi design with grey relational analysis*

The micromachining is executed with the help of micro SECO 905L008-MEGA-T with two flute diameter of 0.8 mm titanium nitride coated tungsten carbide and with KERN Pyramid Ultra precision machining center. Figure 1 shows the experimental setup. The micro milling machine has a maximum rotational speed of 50,000 rpm and a torque of 1.5 N-m. The maximum accuracy and precision are obtained at the temperature of  $20 \pm 5$  °C and humidity of 35%. The tool has a nominal diameter of 800  $\mu\text{m}$ , a  $6 \pm 0.8$   $\mu\text{m}$  cutting edge radius, two flutes, a  $20^\circ$  helix angle and a  $4^\circ$  rake angle. The minimum quantity lubrication is designed with the help of air compressor, infusion pump, pressure regulator and external mix nozzle. The flow rate of nanofluid is at a minimum of 1 mL/h and at a maximum of 1000 mL/h with a precision of 1 mL/h. The nozzle generates a pressure up to air pressure of 6.7 bar and a liquid pressure of 3 bar. The nozzle can deliver the nanofluid up to 250 mm distance without turbulence in the flow. The micro-machining input process parameters selected for conducting the experiment are spindle speed (15000, 30000 and 45000 rpm), feed rate (1, 1.5 and 2 mm), axial depth of cut (0.1, 0.2 and 0.3 mm) and water/x vol.%  $\text{Al}_2\text{O}_3$  ( $x = 1.5, 3$  and  $4.5$ ) nanofluid. The input process parameters selected for this investigation at three levels. The spindle speed is selected based on various literatures and mainly it is decided by the low, medium and high basis of the total spindle speed. By this selection, the influence of spindle speed on response parameters is analyzed accurately. The response parameters selected for this investigation are cutting forces in X( $F_x$ ) and Y( $F_y$ ) directions, tool wear rate (TWR) and surface roughness (SR). The tool wear is determined with the help of SEM (Philips XL30). The cutting forces are identified with the help of Tool dynamometer connected with the Dynoware software. The surface roughness is determined with the help of Mitutoyo Surf Test 301 profilometer [26]. The L9 orthogonal array Taguchi design is selected for conducting the experiment.

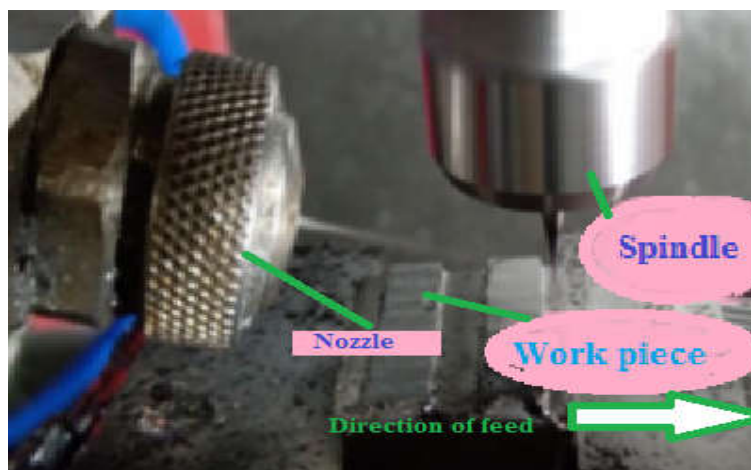


Figure 1. Experimental setup.

The grey relational analysis (GRA) optimization technique is employed to optimize the micro milling process parameters of  $Ti_4Al_4Mo_2Sn$ . The relationship between multiple responses is resolved using GRA analysis [27]. The following steps are used to optimize the micro machining process parameters by using the GRA.

The determination of quality characteristics is done with the help of SN ratio of Taguchi method. Based on the S/N ratio results, three approaches are available such as 'larger is better', 'nominal is better' and 'smaller is better'. The 'smaller is better' approach is employed in this investigation. The surface roughness, tool wear rate and cutting forces are needed to be minimized.

$$S/N_{SB} = -10 \log(1/n \sum_{i=1}^n y_i^2) \quad (1)$$

where  $y_i$  – original sequence.

Several factors are from several resources and they are measured in different units. Therefore, the units of all factors have to be converted into same units. The following equation is used for the attainment of the same unit.

$$Z_{ij} = \frac{y_{ij} - \min(y_{ij, i=1,2,3,\dots,m})}{\max(y_{ij, i=1,2,3,\dots,m}) - \min(y_{ij, i=1,2,3,\dots,m})} \quad (2)$$

where  $y_{ij}$  – data sequence after data processing,  $m$  – experimental data in number and  $n$  – number of responses.

The grey relational coefficient (GRC) is determined to exhibit the relationship between the optimal and normalized experimental results and it is calculated by using the equation

$$y_i^j = \frac{\min_i \min_j |Z_0(i) - Z_j(i)| + \max_j \max_k |Z_0(i) - Z_j(i)|}{|Z_0(i) - Z_j(i)| \max_j \max_k |Z_0(i) - Z_j(i)|} \quad (3)$$

where  $y_i^j$  - grey relational coefficient,  $Z_0i$  - deviation sequence,  $Z_{\min}$  and  $Z_{\max}$  - minimum and maximum values of the absolute differences ( $Z_0i$ ).

Then, the geometric similarity is identified between the series in Grey system and reference series with the help of the Grey Relational Grade. The GRG is calculated using the equation.

$$GRG_{ij} = \frac{1}{n} \sum_{i=1}^n y_i^j \quad (4)$$

where  $GRG_{ij}$  - grey relational grade.

## RESULTS AND DISCUSSION

### *Testing of Water/Al<sub>2</sub>O<sub>3</sub> nanofluids*

The Water/x vol.%  $Al_2O_3$  ( $x = 1.5, 3, 4.5$  and  $6$ ) nanofluids are prepared with the help of the two-step method. The prepared nanofluids are characterized with the help of KD2 thermal property meter and pH meter. The thermal conductivity of the prepared nanofluids is determined with the help of the thermal property meter. The stability of the prepared nanofluids for the duration of 30 days is determined with the help of pH meter and by visual inspection. The prepared Water/4.5 vol.%  $Al_2O_3$  has high dense distribution of  $Al_2O_3$  than the other prepared nanofluids. A high amount of sedimentation occurs in the bottom of the bottle of Water/6 vol.%  $Al_2O_3$  nanofluid. The thermal conductivity of water, Water/1.5 vol.%  $Al_2O_3$ , Water/3 vol.%  $Al_2O_3$ , Water/4.5 vol.%  $Al_2O_3$  and Water/6 vol.%  $Al_2O_3$  are 0.613, 0.637, 0.661, 0.688 and 0.671, respectively and pH value of water, Water/1.5 vol.%  $Al_2O_3$ , Water/3 vol.%  $Al_2O_3$ , Water/4.5 vol.%  $Al_2O_3$  and Water/6 vol.%  $Al_2O_3$  are 7.9, 7.1, 6.75, 6.43 and 6.51, respectively. The increase of  $Al_2O_3$  concentration increases the thermal conductivity up to 4.5 vol.% concentration and decreases by the addition of 6 vol.%. The high thermal conductivity of  $Al_2O_3$  increases the thermal conductivity of nanofluid

[28]. The addition of Al<sub>2</sub>O<sub>3</sub> increases the thermal conductivity of the water based nanofluid and it was already revealed by Kong and Lee [29]. The thermal conductivity of Water/1.38 vol.% Al<sub>2</sub>O<sub>3</sub> is 0.64 and it is lesser than the prepared Water/4.5vol.% Al<sub>2</sub>O<sub>3</sub> nanofluid. The thermal conductivity of Water/4.5vol.% Al<sub>2</sub>O<sub>3</sub> nanofluid is 0.688. The high accumulation of Al<sub>2</sub>O<sub>3</sub> decreases the thermal conductivity of the nanofluid. The sedimentation of Al<sub>2</sub>O<sub>3</sub> occurs at high volume concentration and it causes to decrease the thermal conductivity of the Water/Al<sub>2</sub>O<sub>3</sub> nanofluid [30]. The high accumulation of Al<sub>2</sub>O<sub>3</sub> restricts the flow in the desired direction and temperature of nanofluid increases without dissipation of heat. Another aspect of high accumulation prevents uniform dispersion of the additive in the base fluid which causes to decrease the thermal conductivity. These phenomena cause poor surface finish because of the lower thermal conductivity of the nanofluid which is due to high accumulation. The stability is defined by the occurrence of sedimentation of Al<sub>2</sub>O<sub>3</sub> in the pure water. The stability of Water/x vol.% Al<sub>2</sub>O<sub>3</sub> (x = 0, 1.5, 3, 4.5 and 6) nanofluids are inspected at 30 days, 45 days and 60 days. The sedimentation of Al<sub>2</sub>O<sub>3</sub> in pure water is started after 30 days. The high amount of sedimentation of Al<sub>2</sub>O<sub>3</sub> in pure water occurs at 60 days of the stability test. The sedimentation of Al<sub>2</sub>O<sub>3</sub> in pure water changes the pH value of the nanofluid.

The addition of Al<sub>2</sub>O<sub>3</sub> changes the pH value of the Water/Al<sub>2</sub>O<sub>3</sub> nanofluid. The life of the tool is majorly influenced by the pH value of water/Al<sub>2</sub>O<sub>3</sub> nanofluid. The point of zero surface charge of pure water is between a pH value of 7-8. Therefore, the pH value of pure water is selected as 7.9, which exhibits the optimum thermal conductivity. The point of zero surface charge obtained for pure water is 7.9 pH value. So, pH value of water is selected as 7.9 instead of 7. The point of zero surface charge obtained for Water/Al<sub>2</sub>O<sub>3</sub> is nearly the pH value of 6. The closest pH value for point of zero surface charge is obtained in the combination of Water/4.5 vol.% Al<sub>2</sub>O<sub>3</sub> nanofluid than in the combination of nanofluids. Therefore, the optimum thermal conductivity is obtained in Water/4.5 vol.% Al<sub>2</sub>O<sub>3</sub> nanofluid. The pH value of water does not have much deviation while adding Al<sub>2</sub>O<sub>3</sub> [31].

#### *EDAX and micro structural study*

The EDAX of Al<sub>2</sub>O<sub>3</sub> and Water/x vol. %Al<sub>2</sub>O<sub>3</sub> (x = 1.5, 3 and 4.5) is shown in Figure 2(a-d). The weight percentage of elements presented in the Al<sub>2</sub>O<sub>3</sub> and Water/x vol. %Al<sub>2</sub>O<sub>3</sub> (x = 1.5, 3 and 4.5) is expressed in the EDAX test.

The Figure 2(a-d) represents the EDAX image of purchased Al<sub>2</sub>O<sub>3</sub>, 1.5 wt.% of Al<sub>2</sub>O<sub>3</sub>, 3 wt.% of Al<sub>2</sub>O<sub>3</sub> and 4.5 wt.% of Al<sub>2</sub>O<sub>3</sub>. The increasing wt.% of Al<sub>2</sub>O<sub>3</sub> increases the presence of oxide and aluminum in the nanofluid and it is confirmed from the EDAX test results. The EDAX test results are shown in Table 1.

Table 1. EDAX test results.

Wt.% of Al <sub>2</sub> O <sub>3</sub>	Al %	O %
Purchased Al <sub>2</sub> O <sub>3</sub>	44.18	55.82
1.5wt.% Al <sub>2</sub> O <sub>3</sub>	39.62	60.38
3wt.% Al <sub>2</sub> O <sub>3</sub>	37.91	62.09
4.5 wt.% Al <sub>2</sub> O <sub>3</sub>	31.38	68.62

The microstructure of the Al<sub>2</sub>O<sub>3</sub> and Water/x vol.% Al<sub>2</sub>O<sub>3</sub> (x = 1.5, 3 and 4.5) is shown in Figure 3(a-d). The Figure 3(a) shows the SEM image of the Al<sub>2</sub>O<sub>3</sub> particle and it is in spherical shape. The surface area of the spherical shape is high when compared to other shape of the Al<sub>2</sub>O<sub>3</sub>. The particle shape also enhanced the thermal conductivity of the prepared nanofluid [32]. The Figure 3(b-d) shows the microstructure of Water/x vol.% (x = 1.5, 3 and 4.5). The density of the dispersed Al<sub>2</sub>O<sub>3</sub> is higher in Water/4.5vol.% Al<sub>2</sub>O<sub>3</sub> when compared with the other three combinations and it is justified in the Figure (3d). The Figure 3(b-d) confirms that there is no

sedimentation and accumulation of  $\text{Al}_2\text{O}_3$  in pure water. The TEM images revealed that  $\text{Al}_2\text{O}_3$  particles uniformly dispersed in base fluid. The TEM analysis confirms that uniform distribution of  $\text{Al}_2\text{O}_3$  is achieved in the pure water after nanofluid preparation. The difference between the TEM images of nanofluids is the difference of dense dispersion of  $\text{Al}_2\text{O}_3$  in pure water. The high dense  $\text{Al}_2\text{O}_3$  in pure water is attained in the Water/4.5vol.% of  $\text{Al}_2\text{O}_3$  nanofluid. The uniform dispersion of  $\text{Al}_2\text{O}_3$  enhances the thermal conductivity of the prepared nanofluids [33].

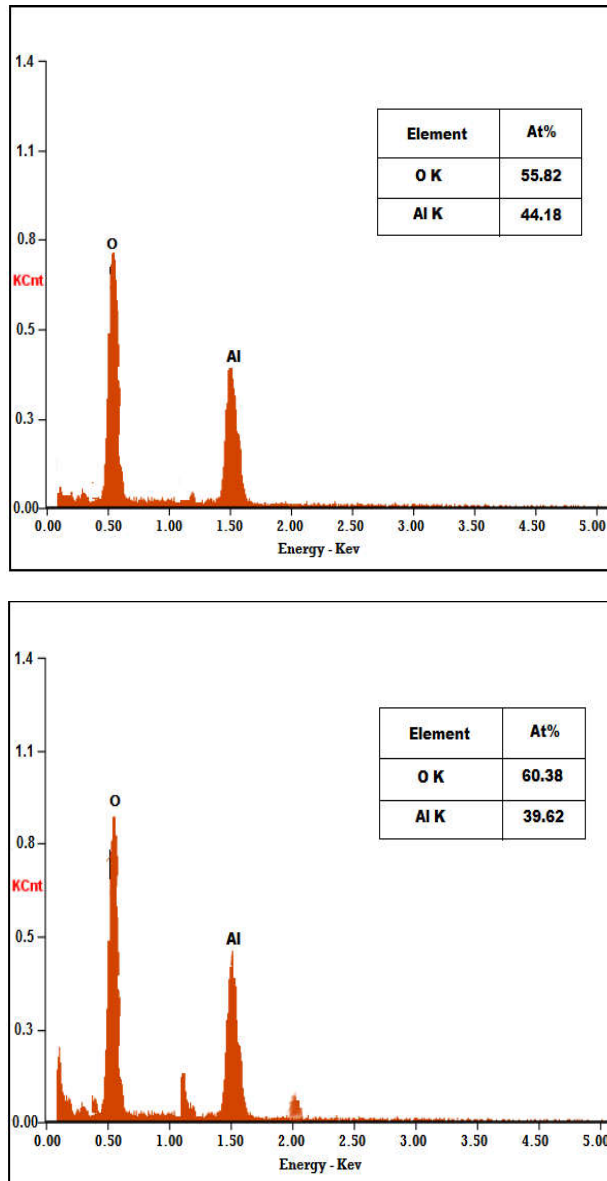


Figure 2. (a) Upper, EDAX of  $\text{Al}_2\text{O}_3$  and (b) lower, EDAX of 1.5vol.%  $\text{Al}_2\text{O}_3$ .

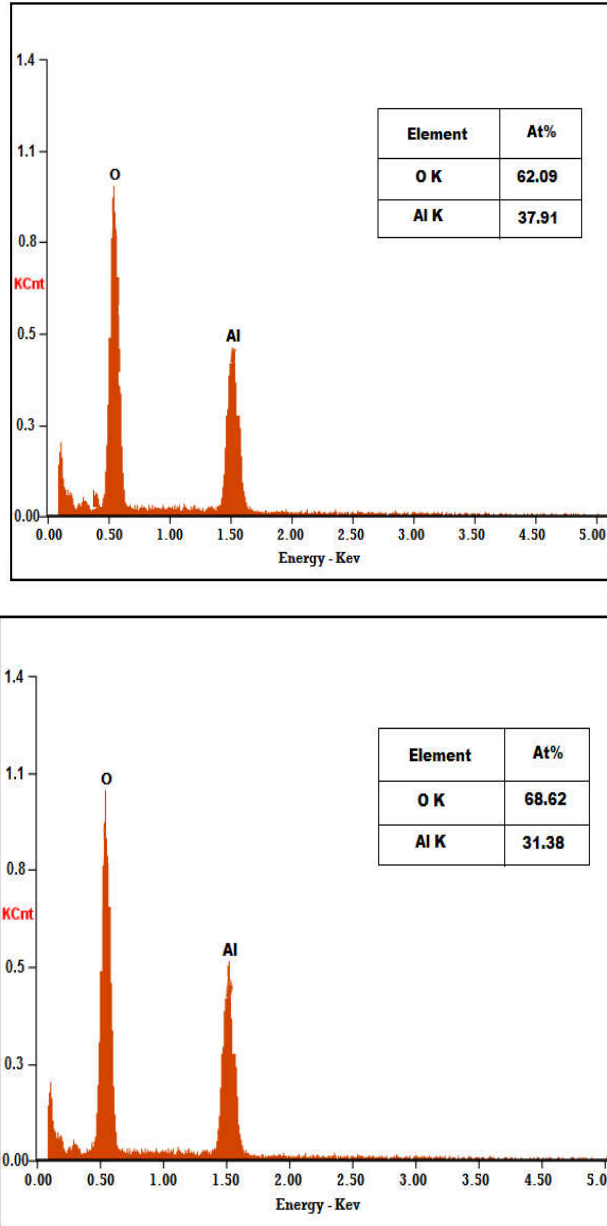


Figure 2. (c) Upper, EDAX of 3vol.%  $Al_2O_3$  and (d) lower, EDAX 4.5vol.%  $Al_2O_3$ .

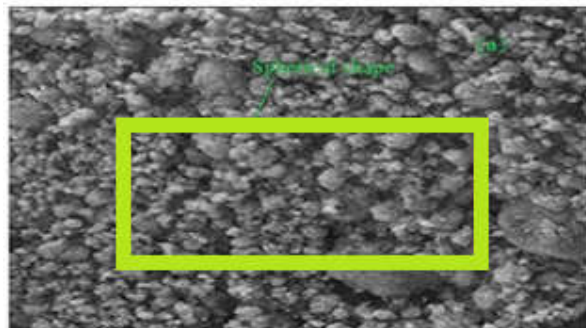


Figure 3(a). SEM image of  $\text{Al}_2\text{O}_3$  at 500 nm.

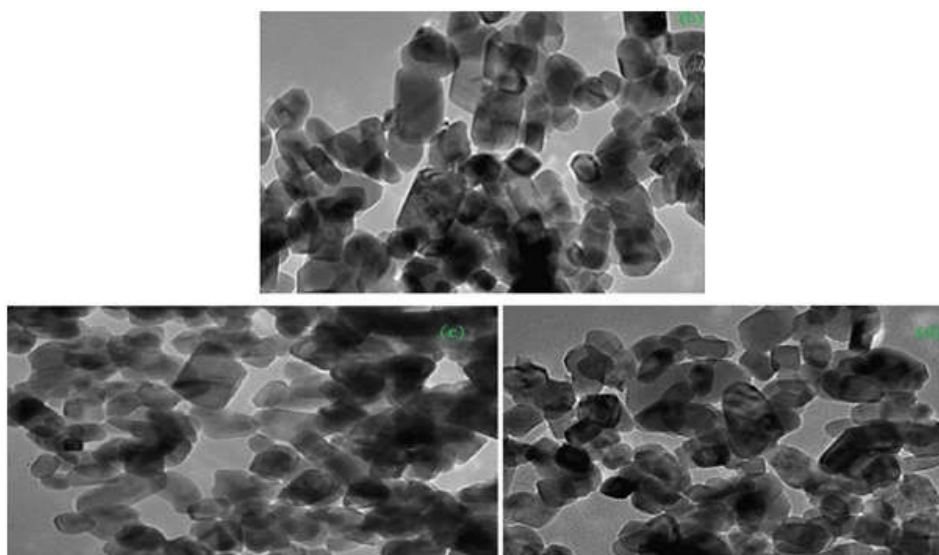


Figure 3(b-d). TEM of Water/vol.%  $\text{Al}_2\text{O}_3$  ( $x = 1.5, 3,$  and  $4.5$ ) at 200 nm.

#### *Taguchi design with GRA optimization*

The grey relational analysis (GRA) multi objective optimization is utilized in this investigation. The Table 2(a) shows the response parameters for its corresponding input process parameters. The experimental data's are used to calculate the grey relational coefficient (GRC) followed by grey relational grade (GRG). The GRG is calculated by taking the average value of GRC. The GRG assessed the effect of the input parameters' change on the response parameters and determined the optimum level of parameters. The highest value of GRG represents better performance of response parameters for its corresponding input process parameters among various experimental runs. The GRC and GRG are calculated with the help of equation 3 and 4.



The highest GRG represents the optimum combination of input process parameters for its response parameters. The Table 2(b) shows the GRC and GRG of experimental trials.

Table 2(a). Experimental results.

TR.NO	A	B	C	D	F <sub>x</sub> (N)	F <sub>y</sub> (N)	TW (μm)	SR (μm)
1	15000	1.0	0.1	1.5	9.50	2.22	28.21	0.06
2	15000	1.5	0.2	3.0	12.47	4.56	59.26	0.15
3	15000	2.0	0.3	4.5	8.13	2.80	31.97	0.16
4	30000	1.0	0.2	4.5	10.81	3.17	23.19	0.08
5	30000	1.5	0.3	1.5	13.01	11.03	52.41	0.12
6	30000	2.0	0.1	3.0	18.19	8.33	24.34	0.14
7	45000	1.0	0.3	3.0	15.29	9.96	33.59	0.08
8	45000	1.5	0.1	4.5	13.85	4.78	18.24	0.18
9	45000	2.0	0.2	1.5	22.42	10.80	26.14	0.11

Table 2(b). Calculation of GRC and GRG.

Run	Evaluation of Δ <sub>0i</sub>				Grey relational coefficient				Grey relational grade	Rank
	F <sub>x</sub>	F <sub>y</sub>	TWR	SR	F <sub>x</sub>	F <sub>y</sub>	TWR	SR	GRG	
1	0.90	1.00	0.76	1.00	0.84	1.00	0.67	1.00	0.70	1
2	0.70	0.73	0.00	0.25	0.62	0.65	0.33	0.40	0.40	7
3	1.00	0.93	0.67	0.17	1.00	0.88	0.60	0.38	0.57	3
4	0.81	0.89	0.88	0.83	0.73	0.82	0.81	0.75	0.62	2
5	0.66	0.00	0.17	0.50	0.59	0.33	0.38	0.50	0.36	9
6	0.30	0.31	0.85	0.33	0.42	0.42	0.77	0.43	0.41	6
7	0.50	0.12	0.63	0.83	0.50	0.36	0.57	0.75	0.44	5
8	0.60	0.71	1.00	0.00	0.56	0.63	1.00	0.33	0.50	4
9	0.00	0.03	0.81	0.58	0.33	0.34	0.72	0.55	0.39	8

The Table 2(b) shows that experimental trial no 1 has the higher GRG among other experimental trials. The 15000 rpm spindle speed, 1 μm feed rate per tooth, 0.1 mm depth of cut and 4.5 vol.% of Al<sub>2</sub>O<sub>3</sub> combination exhibits better performance in the aspect of surface roughness, tool wear and cutting forces. The effect of micro machining process parameters on GRG is shown in Table 3 and is also shown in Figure 4(a-b). The low level of spindle speed, low level of feed rate per tooth, low level of depth of cut and higher concentration of Al<sub>2</sub>O<sub>3</sub> in nanofluid provide the optimum response parameters.

Table 3. Effect of micro machining process parameters on GRG.

Source	L1	L2	L3	Best optimal	Condition	Max-Min	Rank
Spindle speed (A)	<b>0.5585</b>	0.4628	0.4430	<b>0.5585</b>	A1	0.1155	3
Feed rate per tooth (B)	<b>0.5868</b>	0.4222	0.4554	<b>0.5868</b>	B1	0.1646	1
Depth of cut (C)	0.5378	0.4703	0.4563	<b>0.5378</b>	C1	0.0815	4
Al <sub>2</sub> O <sub>3</sub> Nanofluid vol.% (D)	<b>0.4836</b>	0.4151	<b>0.5656</b>	<b>0.5656</b>	D3	0.1505	2

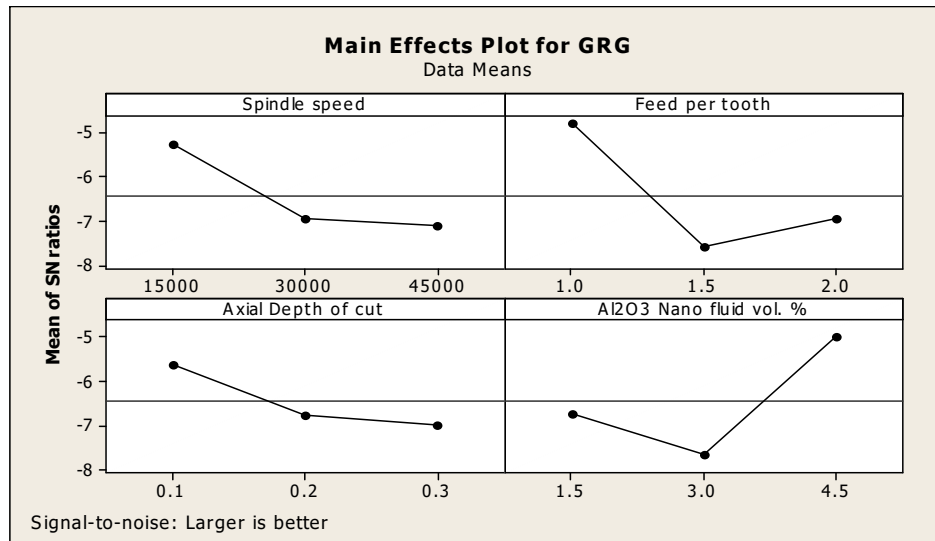


Figure 4(a). Mean effect plot of GRG vs SS, FT, DOC, Al<sub>2</sub>O<sub>3</sub> Vol%.

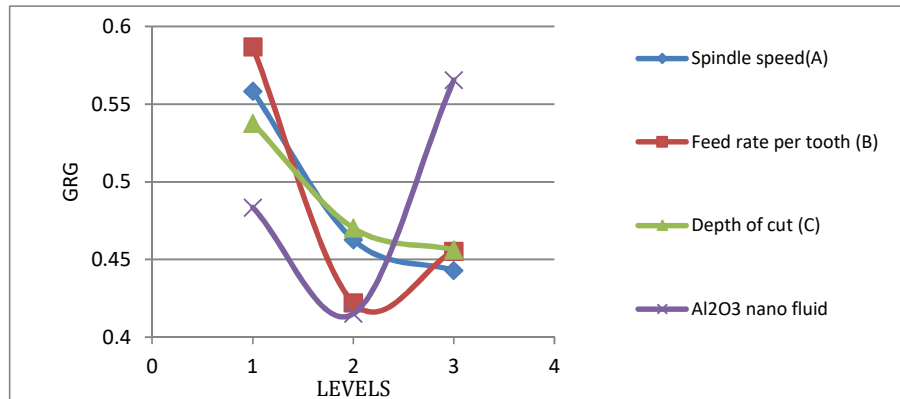


Figure 4(b). Effects of GRG vs levels for SS, FT, DOC, Vol% of Al<sub>2</sub>O<sub>3</sub>.

The influencing parameters sequence obtained from Table 3 is feed rate per tooth, vol.% Al<sub>2</sub>O<sub>3</sub>, spindle speed and depth of cut. The max-min difference shows the importance of individual input process parameters on GRG. The level of individual process parameters of highest grey relational grade represents the optimum process parameters. Analysis of variance is a statistical tool and it is used to investigate the influence of input process parameters on its response parameters. The contribution of each variable on the responses is calculated by ANOVA. The results of grey relational analysis are compared with ANOVA. The ANOVA is shown in Table 4. The input process parameters are significant because p value of all process parameters is less than 0.5 [34]. The contribution percentage of input process parameters are 36.58% feed per tooth, 28.30% spindle speed, 14.27% of Al<sub>2</sub>O<sub>3</sub> vol.% and 14.08% of depth of cut .

Table 4. ANOVA for GRG.

Source	DF	Seq SS	Adj SS	Adj MS	F	P	Contribution %
Spindle speed	4	0.020021	0.0200208	0.0200208	1.67182	0.265639	28.30
Feed per tooth	1	0.025882	0.0258824	0.0258824	2.16130	0.215473	36.58
Axial depth of cut	1	0.009961	0.0099607	0.0099607	0.83176	0.413358	14.08
Al <sub>2</sub> O <sub>3</sub> Nanofluid vol. %	1	0.010080	0.0100804	0.0100804	0.84175	0.410809	14.27
Error	1	0.0047902	0.0479017	0.0119754			6.77
Total	7	0.0707342					100

Table 5. Confirmation test.

Setting	Initial setting A1-B1-C1-D1	Prediction A1-B1-C1-D3	Experimental A1-B1-C1-D3
Tool wear rate	28.21	0.721	23.11
Feed force	9.50		9.43
Normal force	2.22		2.08
Surface roughness	0.06		0.08
GRG	0.70		0.767
Percentage Improvement in GRG	12.46		9.57

The confirmation test is conducted to find the GRG using the equation for these optimum levels and it is shown in Table 5. The percentage of improvement in experimental is 12.46 than its initial setting. The percentage of improvement confirms that the combination of input process parameters significantly improves the grey relational grade from 0.7 to 0.767. The machined surface of work piece material at the condition of A1-B1-C1-D3 is slightly subjected low wear because of Water/4.5vol.% Al<sub>2</sub>O<sub>3</sub> nanofluid with MQL technique. The wear mechanism is abrasion. The work piece material surface has very low surface roughness about 0.7 μm. The low wear in tool and good surface finish in work piece material is achieved by a better heat dissipation using Water/4.5 vol.% Al<sub>2</sub>O<sub>3</sub> nanofluid through MQL technique [35].

## CONCLUSION

The present investigation aimed to investigate the influence of MQL with Water/Al<sub>2</sub>O<sub>3</sub> in the micro machining of Ti<sub>4</sub>Al<sub>4</sub>Mo<sub>2</sub>Sn. The particle size of Al<sub>2</sub>O<sub>3</sub> is measured with the help of PSA and it is 20 nm. The Water/ x vol.% of Al<sub>2</sub>O<sub>3</sub> (x = 1.5,3 and 4.5) nanofluids are prepared with the help of a two-step method. The EDAX and microstructure of prepared nanofluids are studied. The uniform distribution of nano additives is achieved in the prepared nanofluids. The thermal conductivity of Water/4.5 vol.% of Al<sub>2</sub>O<sub>3</sub> is better than the others. The addition of Al<sub>2</sub>O<sub>3</sub> increases the thermal conductivity up to 4.5 vol.% and decreases by the addition of 6 vol.%. The high accumulation of Al<sub>2</sub>O<sub>3</sub> in base fluid decreases the thermal conductivity of the nanofluids. The multi objective optimization is done with the help of L9 Taguchi design with grey relational analysis. The experimental trial no 2 has the highest GRG and it shows a better performance of response parameters with respect to the input process parameters. The ANOVA results show that all factors are significant. The confirmation test is conducted for A1-B1-C1-D3 combination. The GRG percentage of improvement is 12.46. The result of GRA and ANOVA expressed that feed rate per tooth is the most influencing factor. The tool wear is very low and work piece surface finish is better by the implementation of MQL with the Water/4.5 vol.% of Al<sub>2</sub>O<sub>3</sub> nanofluid.

## REFERENCES

1. Zhu, L.; Childs, P.R.N. Light-weighting in aerospace component and system design. *Propuls Power Res.* **2018**, *7*, 103-119.
2. Pramanik, A. Problems and solutions in machining of titanium alloys. *Int. J. Adv. Manuf. Technol.* **2014**, *70*, 5-8.
3. Ingle, S.V.; Raut, D.N. Challenges in machining of titanium alloys with proper tooling and machining parameters - A review. *Int. J. Innov. Eng. Technol.* **2020**, *16*, 25-43.
4. Temitayo, S.O.; Adebunmi, O.; Yussouff, A.; Abideen, O.A. The effects of heat generation on cutting tool and machined workpiece. *J. Phys. Conf. Ser.* **2019**, 1378, 1-10.
5. Musfirah, A.H.; Jaharah, A.; Ghani C.H.; Cheharon, S. Tool wear and surface integrity of inconel 718 in dry and cryogenic coolant at high cutting speed. *Wear* **2017**, *377*, 125-133.
6. Abu, R.; Ali Bodius, S. A review on nanofluid: Preparation, stability, thermophysical properties, heat transfer characteristics and application. *SN Appl. Sci.* **2020**, *2*, 1-12.
7. Ravisankar, B.; Tara, C. Influence of nanoparticle volume fraction, particle size and temperature on thermal conductivity and viscosity of nanofluids - A review. *Int. J. Automot. Mech. Eng.* **2013**, *8*, 1316-1338.
8. Jia-Fei, Z.; Zhong, Y.; LuoMing, J.; NiKe-Fa, C. Dependence of nanofluid viscosity on particle size and pH value. *Chin. Phys. Lett.* **2009**, *26*, 1-14.
9. Hans, M.R. A transient hot wire thermal conductivity apparatus for fluids. *J. Res. Natl. Bur. Stand.* **1981**, *86*, 457-493.
10. Mehrdad, K.; Mostafa, S.; Kürşat, Ş.; Pinar, M. The effect of nanoparticle type and nanoparticle mass fraction on heat transfer enhancement in pool boiling. *Int. J. Heat Mass Transf.* **2017**, *109*, 157-166.
11. Vicki, W.; Abdullah, M.Z.; Gunnasegarana, P. Effect of TiO<sub>2</sub> -Al<sub>2</sub>O<sub>3</sub> nanoparticle mixing ratio on the thermal conductivity, rheological properties, and dynamic viscosity of water-based hybrid nanofluid. *J. Mater. Res. Technol.* **2020**, *9*, 13781-13792.
12. Yusuf, K.; Armin, G.; Umit, Y.; Uğur, K. A comparison of flood cooling, minimum quantity lubrication and high pressure coolant on machining and surface integrity of titanium Ti-5553 alloy. *J. Manuf. Process.* **2018**, *34*, 45-51.
13. Hegab, H. On machining of Ti-6Al-4V using multi-walled carbon nanotubes-based nano-fluid under minimum quantity lubrication. *Int. J. Adv. Manuf. Technol.* **2018**, *45*, 1-11.
14. Hegab, H. Performance evaluation of Ti-6Al-4V machining using nano-cutting fluids under minimum quantity lubrication. *Int. J. Adv. Manuf. Technol.* **2018**, *95*, 4229-4241.
15. Vipin, N.A.; Parekh, S.; Tailor, P.R. Water-based Al<sub>2</sub>O<sub>3</sub>, CuO and TiO<sub>2</sub> nanofluids as secondary fluids for refrigeration systems: A thermal conductivity study. *J. Braz. Soc. Mech. Sci.* **2018**, *40*, 1-10.
16. Shrikant, S.; Dhurgude, P. Review on influence of cooling technique on tool wear in turning of titanium alloy Ti-6Al-4V. *Int. J. Eng. Technol.* **2017**, *4*, 1-14.
17. Srinivasan, L.; Chand, K.M.; Kannan, T.D.; Sathiya, P.; Biju, S. Application of GRA and TOPSIS optimization techniques in GTA welding of 15CDV6 aerospace material. *Trans. Indian Inst. Metals* **2018**, *71*, 373-382.
18. Çakır, A.; Yağmur, S.; Kavak, N.; Şeker, U. The effect of minimum quantity lubrication under different parameters in the turning of AA7075 and AA2024 aluminum alloys. *Int. J. Adv. Manuf. Technol.* **2015**, *12*, 1-16.
19. Paul, G.; Philip, J.; Raj, B.; Das, P.K.; Manna, I. Synthesis, characterization, and thermal property measurement of nano-Al<sub>195</sub>Zn<sub>05</sub> dispersed nanofluid prepared by a two-step process. *Int. J. Heat Mass Transf.* **2011**, *54*, 3783-3788.
20. Chen, H.; Ding, Y.; Lapkin, A. Rheological behaviour of nanofluids containing tube/rod-like nanoparticles. *Powder Technol.* **2009**, *194*, 132-141.

21. Vajjha, R.S.; Das, D.K. Experimental determination of thermal conductivity of three nanofluids and development of new correlations. *Int. J. Heat Mass Transf.* **2009**, *52*, 4675-4682.
22. Azmi, W.H.; Sharma, K.V.; Mamat, R.; Najafi, G.; Mohamad, M.S. The enhancement of effective thermal conductivity and effective dynamic viscosity of nanofluids – A review. *Renew. Sust. Energ. Rev.* **2016**, *53*, 1046-1058.
23. Malik, B.; Endarko, E.; Triwikantoro, T. Particle Size Analysis of the synthesized Al<sub>2</sub>O<sub>3</sub> by dissolution and alkali fusion-coprecipitation methods. *Key Eng. Mater.* **2020**, *860*, 1-14.
24. Muhammad, Rafiq, M.; Lv, Yuzhen; Li, C. A review on properties, opportunities, and challenges of transformer oil-based nanofluids. *J. Nanomater.* **2016**, *4*, 1-23.
25. Pravin, D.N.; Vigneshwaran, V. Stability and thermal conductivity studies of MWCNTs nanofluids stability and thermal conductivity studies of MWCNTs nanofluids. *Int. J. Res.* **2018**, *15*, 45-52.
26. Vishal, S.; Sharma, S.D.; Rakesh, S.; Sharma, S.K. Estimation of cutting forces and surface roughness for hard turning using neural networks. *J. Intell. Manuf.* **2008**, *19*, 473-483.
27. Prasanth, A.; Sylajakumari, R.; Gopalakrishnan, P. Taguchi grey relational analysis for multi-response optimization of wear in Co-continuous composite. *MDPI* **2018**, *11*, 1-17.
28. Khamisah, A.H.; Azmi, W.H.; Rizalman, M.; Usri, N.A. Thermal conductivity enhancement of aluminum oxide nanofluid in ethylene glycol. *Appl. Mech. Mater.* **2014**, *660*, 1-14.
29. Kong, M.; Lee, S. Performance evaluation of Al<sub>2</sub>O<sub>3</sub> nanofluid as an enhanced heat transfer fluid. *Adv. Mech. Eng.* **2020**, *12*, 1-13.
30. Mostafa, M.; Sina Razvarz, K. Experimental investigation of aluminum oxide nanofluid on heat pipe thermal performance. *Int. Commun. Heat Mass Transf.* **2012**, *39*, 1444-1448.
31. Junyu, J.; Xiangyang, Y.; Jun, G.; Wei, L. Effect of surfactants and pH values on stability of  $\gamma$ -Al<sub>2</sub>O<sub>3</sub> nanofluids. *Chem. Phys. Lett.* **2018**, *781*, 78-85.
32. Jisun, J.; Li, C.; Younghwan, K.; Jaekun, L. Particle shape effect on the viscosity and thermal conductivity of ZnO nanofluids. *Int. J. Refrig.* **2016**, *36*, 2233-2241.
33. Singh, K. Thermal conductivity of nanofluids. *Def. Sci. J.* **2014**, *58*, 600-607.
34. Balamurugan, G.; Biswanath, M.; Sukamal, G. Taguchi method and ANOVA: An approach for process parameters optimisation of hard machining while machining hardened steel. *J. SciInd. Res. (India)* **2009**, *68*, 686-695.
35. Vasu, V. Effect of minimum quantity lubrication with Al<sub>2</sub>O<sub>3</sub> nanoparticles on surface roughness, tool wear and temperature dissipation in machining Inconel 600 alloy. *Proc. Inst. Mech. Eng. N: J. Nanomater. Nanoeng. Nanosyst.* **2011**, *225*, 3-11.